Nanoscale

c3nr03016d

PAPER

1

Resonance energy transfer in self-organized organic/inorganic dendrite structures

D. Melnikau, D. Savateeva, V. Lesnyak, N. Gaponik, Y. Núnez Fernández, M. I. Vasilevskiy, M. F. Costa, K. E. Mochalov, V. Oleinikov and Y. P. Rakovich

Förster-type coupling is demonstrated for self-assembled dendrite structures consisting of J-aggregates and QDs, with energy fluxes directed towards structures' center.

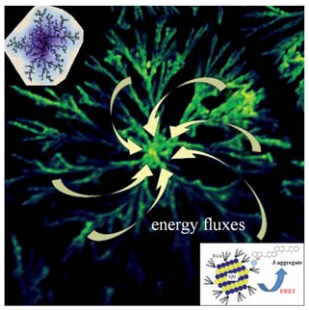

Please check this proof carefully. **Our staff will not read it in detail after you have returned it**.

Translation errors between word-processor files and typesetting systems can occur so the whole proof needs to be read. Please pay particular attention to: tabulated material; equations; numerical data; figures and graphics; and references. If you have not already indicated the corresponding author(s) please mark their name(s) with an asterisk. Please e-mail a list of corrections or the PDF with electronic notes attached – do not change the text within the PDF file or send a revised manuscript. Corrections at this stage should be minor and not involve extensive changes. All corrections must be sent at the same time.

Please bear in mind that minor layout improvements, e.g. in line breaking, table widths and graphic placement, are routinely applied to the final version.

We will publish articles on the web as soon as possible after receiving your corrections; **no late corrections will be made.**

Please return your **final** corrections, where possible within **48 hours** of receipt by e-mail to: nanoscale@rsc.org

Queries for the attention of the authors

Journal: **Nanoscale**

Paper: **c3nr03016d**

Title: **Resonance energy transfer in self-organized organic/inorganic dendrite structures**

Editor's queries are marked like this...**1**, and for your convenience line numbers are inserted like this... 5

Please ensure that all queries are answered when returning your proof corrections so that publication of your article is not delayed.

Query Reference	Query	Remarks
1	For your information: You can cite this article before you receive notification of the page numbers by using the following format: (authors), Nanoscale, (year), DOI: 10.1039/c3nr03016d.	
2	Please carefully check the spelling of all author names. This is important for the correct indexing and future citation of your article. No late corrections can be made.	
3	Do you wish to indicate the corresponding author(s)?	

Nanoscale

RSC Publishing

PAPER

Resonance energy transfer in self-organized organic/inorganic dendrite structures

Cite this: DOI: 10.1039/c3nr03016d

D. Melnikau,[ab] D. Savateeva,[a] V. Lesnyak,[c] N. Gaponik,[d] Y. Núnez Fernández,[e] M. I. Vasilevskiy,[e] M. F. Costa,[e] K. E. Mochalov,[fg] V. Oleinikov[fg] and Y. P. Rakovich[ah]

Received 11th June 2013
Accepted 23rd July 2013

DOI: 10.1039/c3nr03016d

www.rsc.org/nanoscale

Hybrid materials formed by semiconductor quantum dots and J-aggregates of cyanine dyes provide a unique combination of enhanced absorption in inorganic constituents with large oscillator strength and extremely narrow exciton bands of the organic component. The optical properties of dendrite structures with fractal dimension 1.7–1.8, formed from J-aggregates integrated with CdTe quantum dots (QDs), have been investigated by photoluminescence spectroscopy and fluorescence lifetime imaging microscopy. Our results demonstrate that (i) J-aggregates are coupled to QDs by Förster-type resonant energy transfer and (ii) there are energy fluxes from the periphery to the centre of the structure, where the QD density is higher than in the periphery of the dendrite where the density is lower. Such an anisotropic energy transport can be only observed when dendrites are formed from QDs integrated with J-aggregates. These QD/J-aggregate hybrid systems can have applications in light harvesting systems and optical sensors with extended absorption spectra.

Introduction

Hybrid organic/inorganic nanostructures are promising materials with unique optical, electrical and photophysical properties, which can be very different from those of their constituent parts. Self-assembly processes offer a route for assembling these hybrid nanomaterials into larger functional systems, providing a platform for future applications in nano- and optoelectronic devices, nanomanufacturing, renewable energy harvest and storage, biomedical sensing, *etc.*[1–4]

Recent reports on hybrid nanostructures based on semiconductor quantum dots (QDs) and organic cyanine dyes (J-aggregates) demonstrate that they are very promising for photovoltaic applications where QD/J-aggregate complexes could work as extremely efficient light-harvesting antennas with a strongly extended spectral absorption range.[5–7] Therefore, the development of a novel organic/inorganic hybrid material by combining QDs and J-aggregates and exploring the effect of excitonic energy transfer between confined Wannier–Mott excitons of inorganic semiconductor structures and Frenkel excitons of organic dyes (or their aggregates) are of considerable interest for fundamental studies of interaction between light and matter.[8] Apparently the efficiency of light-harvesting by QD/J-aggregate complexes can be further enhanced by organizing them into self-assembled dendritic structures due to the effective energy transport from the strongly light-absorbing periphery to the core of the dendrites like it was shown for pure QD dendritic structures.[9] Organization of these hybrid materials into self-assembled organic/inorganic dendrites is also an important advancement with the potential for far-reaching and industrial applications.

It is well known that under certain conditions, different types of QDs can form dendritic structures of various sizes and shapes.[9–11] Despite the fact that the dendritic structures are formed spontaneously, their size and shape can be controlled by changing the concentrations of the components in solution and the rate of liquid evaporation.[9,10] In our previous work[7] we have shown the possibility to create a complex network superstructure, which consists of QD/J-aggregate building blocks with highly efficient non-radiative energy transfer properties. In the present work, the aim was to investigate the possibility of further enhancement of the efficiency of light-harvesting by QD/J-aggregate complexes by organizing them into self-assembled dendritic structures. We expected to find experimental and theoretical evidence for the effective energy transport from the strongly light-absorbing periphery to the core of the dendrites, taking place because of the fractal nature of the dendrites.

[a]Centro de Física de Materiales (MPC, CSIC-UPV/EHU), Donostia International Physics Center (DIPC), Po Manuel de Lardizabal 5, Donostia-San Sebastian 20018, Spain. E-mail: yury.rakovich@ehu.es
[b]CIC nanoGune Consolider, Tolosa Hiribidea 76, Donostia-San-Sebastian, 20018, Spain
[c]Istituto Italiano di Tecnologia, Via Morego 30, 16163 Genova, Italy
[d]Physikalische Chemie, TU Dresden, 01062 Dresden, Germany
[e]Centro de Física and Departamento de Física, Universidade do Minho, Campus de Gualtar, Braga 4710-057, Portugal
[f]Laboratory of Nano-Bioengineering, Moscow Engineering Physics Institute, 115409 Moscow, Russian Federation
[g]Shemyakin-Ovchinnikov Institute of Bioorganic Chemistry Russian Academy of Sciences, 117997 Moscow, Russian Federation
[h]IKERBASQUE, Basque Foundation for Science, Bilbao 48011, Spain

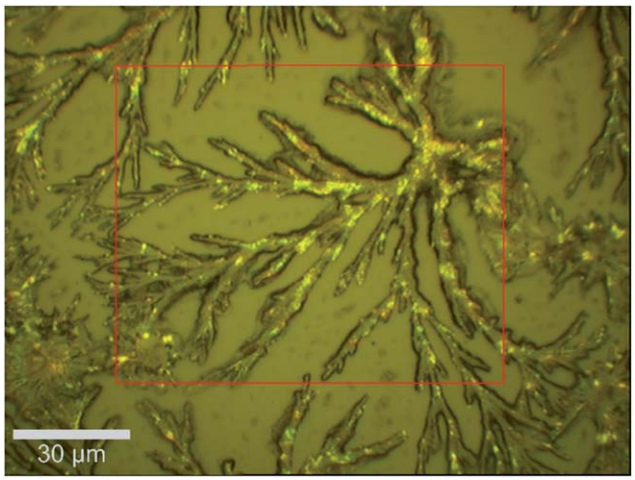

Fig. 1 Microscopic image of a dendrite formed by CdTe QDs mixed with J-aggregates.

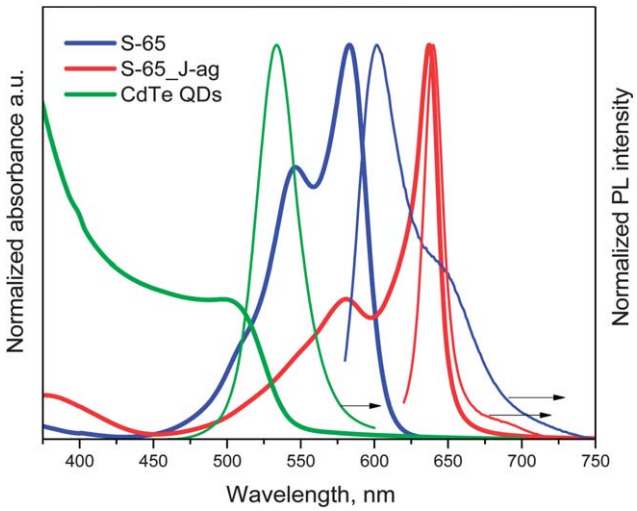

Fig. 2 Room-temperature absorption and PL spectra of QDs (green, $\lambda_{exc.}$ = 450 nm), non-aggregated S-65 dye (blue, $\lambda_{exc.}$ = 560 nm), and its J-aggregates (red) formed in aqueous solution of S-65 by interaction with the PEI polyelectrolyte (Sigma-Aldrich), ($\lambda_{exc.}$ = 600 nm).

Then, intuitively, one can expect an anisotropy in the energy fluxes to and from the centre of the structure, where the QD density is higher than that in the periphery of the dendrite. Recently this effect has been shown for dendritic structures made from pure QDs of two different sizes.[9] Therefore we investigate the feasibility of using hybrid nanostructures consisting of QDs and J-aggregates for the formation of artificial light harvesting and light emitting systems, namely, dendrites composed of CdTe QDs decorated with J-aggregates of cyanine dye, an example of which is shown in Fig. 1.

Experimental details

CdTe quantum dots were synthesized in an aqueous solution using thioglycolic acid (TGA) as the capping agent.[12,13] CdTe QDs capped with TGA carry a negative charge and have emission centered at 533 nm (Fig. 2). This emission maximum corresponds to an average QD size of 2.2 nm, as estimated from the sizing curve provided by Rogach *et al.*[12]

J-aggregates were formed from the S2165 (S-65) dye 2-[3-[1,1-dimethyl-3-(4-sulfobutyl)-1,3-dihydro-benzo[*e*]indol-2-ylidene]-propenyl]-1,1-dimethyl-3-(4-sulfobutyl)-1*H*-benzo[*e*]indolium hydroxide. Hybrid structures of QDs and the J-aggregates were produced by the addition of the concentrated 10^{-3} mol L^{-1} water solution of the S-65 dye to an aqueous solution of 10^{-5} mol L^{-1} CdTe QDs at a volume ratio of 1 : 10 in the presence of NaOH pH = 11. A high pH value is required to stabilize the QDs at a low concentration. 1–2 μL aliquots of aqueous solution of hybrid QD/J-aggregates were deposited on the object glass and allowed to dry. Most of the drying experiments were performed in an ambient atmosphere at room temperature (20–25 °C). Doubly purified deionized water from an 18 MU Millipore system was used for all dilutions.

At the initial stage of droplet drying (at a sufficiently high concentration of the nanocrystals) first a thick boundary layer is formed which consists of completely non-aligned nanocrystals. As the formation of this layer goes on, both the concentration of the nanocrystals in a droplet and the rate of their delivery to the border decrease which provides the conditions for the alignment of the nanocrystals and the beginning of the formation of a dendrite structure. At this point the electrostatic interaction between positively charged nitrogen atoms of the dye and negatively charged carboxylic groups on the surface of the quantum dots stimulates formation of rod-shaped J-aggregates which, in turn, promotes formation of branches of a dendrite.

Cary 50 (Varian) and FP6600 (Jasco) were used to measure the absorption and photoluminescence (PL) spectra, respectively. A confocal Raman microscopy setup (Alpha300, WITec: 600 and 1800 mm^{-1} gratings, with >3 and >1 cm^{-1} spectral resolution, respectively) was used to measure micro-PL spectra in a backscattering geometry. A continuous wave laser emitting at 532 nm was used in the micro-PL measurements. The time resolved PL decays were recorded using a PicoQuant Microtime200 time resolved confocal microscope system, equipped with an Olympus IX71 inverted microscope. The samples were excited by a 405 nm or by a 485 nm picosecond laser pulse (PicoQuant LDH-405 and DH485 laser heads controlled by Sepia II driver). The system has an overall resolution of 100 ps. PL lifetime maps (two-dimensional in-plane variations of the PL decay times) were calculated on a per pixel basis by fitting the lifetime of each pixel to the logarithm of the intensity.

Experimental results and discussion

Optical properties of uncoupled QDs and J-aggregates

The absorption and PL spectra of CdTe QDs and S-65 dye are presented in Fig. 2. The absorption spectrum of the non-aggregated S-65 dye consists of a well-defined monomeric peak centered at 583 nm and vibrational progressions of two modes at 547 and 507 nm. It is noteworthy that the PL spectrum of S-65 does not completely mirror the absorption spectrum in the range of the first vibrational band. Therefore from the

comparison of the absorption and fluorescence spectra of S-65 in water, the presence of associates or H-aggregates, whose absorption overlaps with the vibrational band at 547 nm, was assumed.

J-aggregates of S-65 show a narrow absorption band at 637 nm and a strong fluorescence band with a Stokes shift between them of only 3 nm (Fig. 2). It should be noted that the position of the absorption and fluorescence maxima of J-aggregates to some extent depends on the polyelectrolyte or salt that triggers the formation of J-aggregates of S-65. CdTe QDs emit in the spectral region of the maximum of S-65 monomer absorption providing good conditions for Förster resonant energy transfer (FRET). At the same time, their PL band is located far from the fluorescence of the monomer and J-aggregate bands of the dye, which allows us to determine the contribution of each component to the total fluorescence spectrum of hybrid nanostructures. These optical properties of QDs and J-aggregates give us the opportunity to develop an efficient hybrid material working in the FRET regime.

The formation of J-aggregates of S-65 required the addition of polyethyleneimine (PEI) or poly(diallyldimethylammonium-chloride) (PDDA). In our previous work[7] we demonstrated that formation of J-aggregates in an aqueous solution of cationic cyanine dye pseudoisocyanine iodide (PIC) can be induced by direct injection of QDs capped with TGA carrying a negative surface charge without the need for any further surface functionalization. In other words, QDs serve as a template for J-aggregate formation. Electrostatic interactions between the cationic sites of the S-65 dye molecule and anionic groups of the TGA stabilizing surface of QDs stimulate J-aggregate formation of the S-65 dye in the same way as it has been shown before[6,7] for cyanine dyes PIC and TTBC, respectively.

Dendrite structures

We investigated the topological structure of the dendrites by analysing their spectral microscopy images (such as the one shown in Fig. 1), as well as the PL intensity maps (Fig. 4a). The box-counting algorithm[14] was used for calculation of the fractal dimension. After application of basic image enhancement thresholding and binarization operators, the binary images were covered with different grids (box lengths ε). The number of boxes, $N(\varepsilon)$, required to cover the structures of the fractal image was recorded. If an object is an ideal fractal, $N(\varepsilon)$ increases according to the relationship:

$$N(\varepsilon) = C\varepsilon D \quad (1)$$

where D is the fractal dimension and C is a constant. From eqn (1) the fractal dimension D can be derived as:

$$D = \lim_{\varepsilon \to 0}[-\log N(\varepsilon)/\log \varepsilon] \quad (2)$$

i.e., it is the slope of a double-logarithmic plot of $N(\varepsilon)$ against ε. For instance, for the microscopic image in Fig. 1, we obtained $D \approx 1.71$. Interestingly, the algorithm yields a similar value of 1.74 for the PL intensity map of the same sample (Fig. 4a).

As previously reported, the addition of various components to the solution of QDs can also change the structure and shape of QD based dendrites formed during the evaporation of the solution.[10] Therefore, dendritic structures formed by QD/J-aggregate hybrid materials may be different from pure QD dendrites, despite the fact that the same conditions were used for dendrite growth. As a rule, dendrites formed by QD/J-aggregate hybrid materials are smaller than those formed by QDs alone, however, by changing the rate of liquid evaporation and the affinity of the substrate we can control the shape and size of the dendrites.

Optical properties of the dendrites

First, in order to determine the distribution of non-aggregated dye molecules and J-aggregates on the surface of the hybrid QD/J-aggregate dendrite we measured micro-PL spectra from spots (1×1 μm in area) located in different parts of the dendrite, using the 532 nm laser excitation (see Fig. 3). The maximum of the PL spectrum of QD/J-aggregates at 634 nm, presented in Fig. 3, certainly belongs to the J-aggregates' emission, while the small shoulder at 605 nm is caused by the fluorescence of the monomer dye S-65. Another small shoulder around 540 nm belongs to the QD emission cut off by the filter of our confocal microscopy setup.

Based on these spectra, we conclude that the dye in the monomeric form is uniformly distributed over the entire surface of the sample, while the J-aggregates are mainly localized within the dendritic structures formed by QDs, presumably due to the fact that the QDs serve as a template for J-aggregate formation. In this scenario, J-aggregates first cover the surface of the QDs in solution and then dendrite structures are formed by hybrid QD/J-aggregates.

FLIM images obtained by PL decay mapping of the dendritic structures of QDs and of hybrid QD/J-aggregate structures are presented in Fig. 4. The corresponding PL kinetics (not shown) present a multi-exponential PL decay, which is typical for different types of QDs.[15] From their analysis we can distinguish

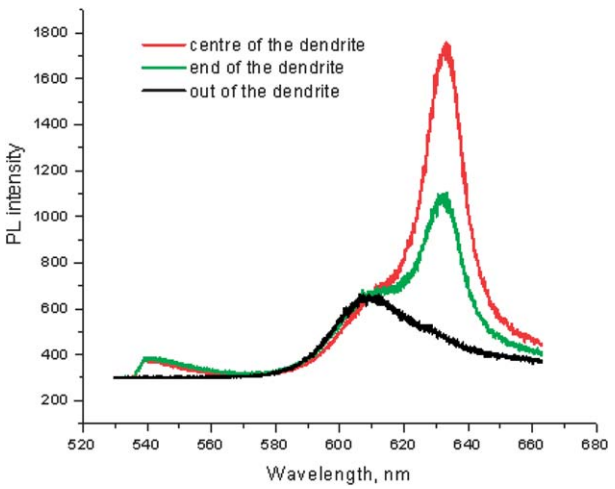

Fig. 3 PL spectra from different dendrite spots, located in the centre of the dendrite (red), in its periphery (green) and outside of the dendrite (black). The laser excitation wavelength is 532 nm.

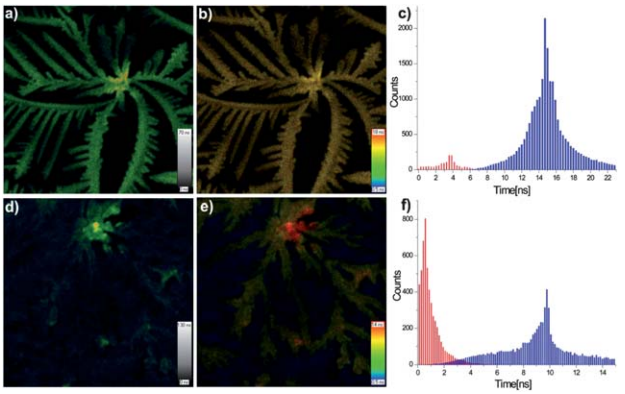

Fig. 4 PL intensity (a and d) and PL lifetime (b and e) maps, for pure CdTe QD dendrites (a and b) and QD/J-aggregate dendrites (d and e), respectively. The corresponding PL lifetime histograms (c and f) were obtained by means of two-exponential fitting of the PL decay kinetics at each image spot while scanning over a 60 × 60 μm area. The bar heights represent the relative statistical weights of the two components (τ_1 and τ_2). The laser excitation wavelength is 480 nm.

two characteristic times, τ_1 and τ_2 ($\tau_2 > \tau_1$), represented by red and blue colors, respectively, in the histograms of Fig. 4.

Both τ_1 and τ_2 show some statistical distributions, which can be caused by size dispersion of QDs and/or variation of the energy levels of shallow traps at the surface of QDs. Fig. 4 clearly demonstrates shortening of the lifetime of the two components for hybrid structure QD/J-aggregates, compared to the pure QD dendrite (see Fig. 4c and f). At the same time, a significant increase in the relative weight of the τ_1 component is seen in the presence of J-aggregates. Clearly, we do not have just a simple overlapping of the τ_1 and τ_2 distributions of the QDs and J-aggregates. It means that the two species in the hybrid QD/J-aggregates are coupled, *i.e.* they are in the FRET regime.

Looking at the maps of Fig. 4, for both pure QD and hybrid QD/J-aggregate dendritic structures one can see a highly luminescent core which corresponds to the center of the fractal structure. At the same time, in contrast to the pure QD dendrite, for the hybrid structure a pronounced inhomogeneity in the lifetime spatial distribution, with longer PL lifetimes (τ_2), at the core of the dendrite is observed. While the non-uniform distribution of the emission intensity may reflect just the higher density of the emitters in the core region, the inhomogeneity in the lifetime cannot be explained in this way and indicates that energy transfer processes take place in the structure, making the lifetime dependent on the local environment within the self-assembled structure.

Both J-aggregates and monomers of S-65 show efficient photoluminescence when excited at wavelengths within their absorption bands. In the FRET regime, the significantly increased absorption of the hybrid QD/J-aggregate system in the blue and UV spectral regions provides a possibility for efficient pumping of the J-aggregates' PL using an excitation wavelength near 400 nm where the absorption of both the dye monomer and J-aggregates is minimal. Therefore, in order to be sure that we do not excite directly the non-aggregated dye, we used a 405 nm laser light source and monitored changes in the PL lifetime distribution for the hybrid QD/J-aggregate dendrite system (Fig. 5). Likewise for the 480 nm excitation (see Fig. 4), with the 405 nm laser, we observe a shortening of the PL lifetime for the hybrid QD/J-aggregate structure, compared to the pure QD one (the peak of the τ_2 distribution shifts from 18 to 15 ns). Consistently, the lifetime (τ_2) and the emission intensity for the hybrid structures change from the periphery to the core of the dendrite (Fig. 5d–f). Since the luminescence band of J-aggregates is red-shifted by more than 100 nm, compared to the PL band of QDs, we cut off the luminescence of QDs using an appropriate narrow band filter and evaluated the efficiency of excitation of the J-aggregates through the energy transfer from the QDs. The PL intensity and FLIM maps of the hybrid dendritic structures obtained this way (using an appropriate cut off filter) are presented in Fig. 5g and h.

We notice that the intensity of J-aggregates' emission, *excited only indirectly through QDs* and measured under these conditions, is just 4 times lower than for the same dendrite in the case where no filter was used (compare Fig. 5f and i). The J-aggregates' luminescence caused by the 405 nm excitation is only possible due to the QD absorption in the UV/blue spectral region (see Fig. 2), followed by the efficient energy transfer from QDs to J-aggregates. On the basis of comparison of the PL lifetimes and intensity of QDs alone and in the presence of J-aggregates, under the 405 nm excitation, we can estimate that the efficiency of FRET from the QDs to J-aggregates is higher than 30–40%.

However, it is not sufficient to explain the longer fluorescence lifetime in the central part of the dendrite, compared to the periphery, as clearly seen in Fig. 4e and 5e. Independent of the excitation wavelength, for hybrid QD/J-aggregate dendritic structures we observe this inhomogeneous spatial distribution of the lifetime (τ_2 – represented by red colour in Fig. 5) over the area of the dendrite. We have to presume that there are also Förster type processes transporting energy, mostly from the periphery to the core region of the dendrite. In the next section we present modeling results, which show that these processes, owing to the fractal geometry of the dendrite structures, indeed can lead to the inhomogeneity of the excitation lifetime.

Modelling results

First, we generated fractal aggregates of particles that mimic the experimentally studied dendrites with the dimensionality $D \approx 1.7 \div 1.8$, which is close to the value known for clusters obtained by the so-called diffusion-limited aggregation (DLA).[16] We assume that the particles forming DLA dendrites are some identical light emitting and absorbing entities, which are coupled by reversible Förster-type energy transfer processes, with the probability per unit time given by

$$W_{i\to j} = \tau^{-1}\left(\frac{R_F}{r_{ij}}\right)^6 \quad (3)$$

where the indices i and j refer to any two of the particles, τ is the radiative lifetime, R_F is the Förster radius and r_{ij} is the inter-particle distance. The polarization of an array of such particles should be calculated as a function of time. The probability to

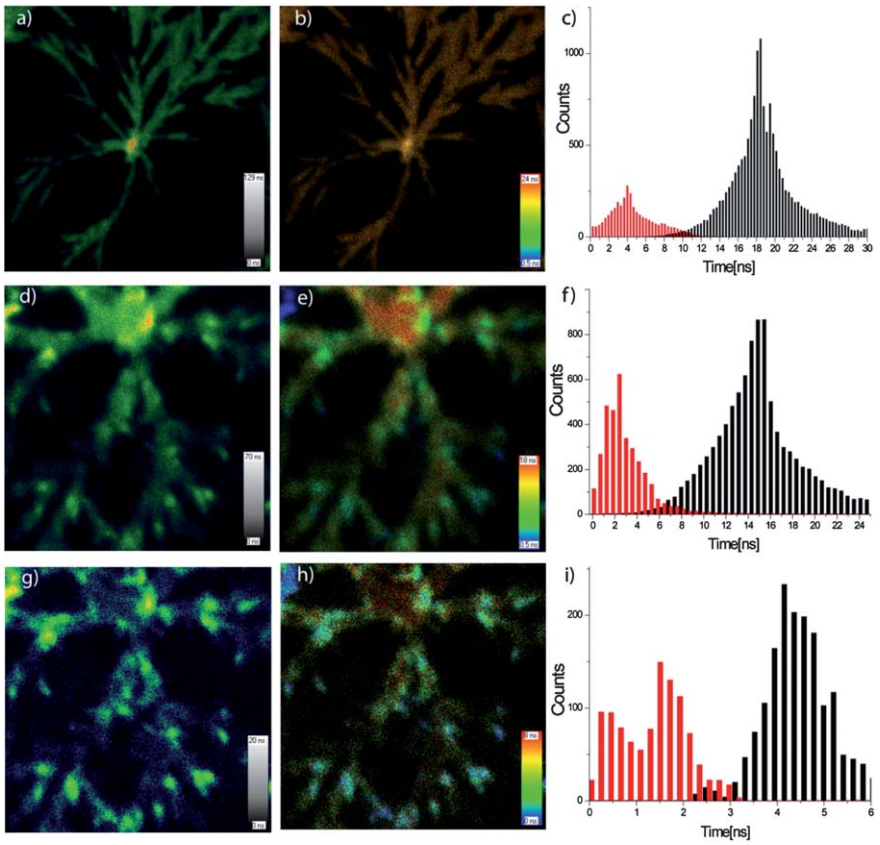

Fig. 5 PL intensity (a, d, and g), PL lifetime images (b, e, and f) and corresponding PL lifetime histogram (c, f, and i) of a pure CdTe QD dendrite (top), a QD/J-aggregate dendrite (middle), a QD/J-aggregate dendrite (bottom) with a narrow band filter cutting the luminescence of QDs. Excitation wavelength is 405 nm.

find the i-th particle polarized (*i.e.* excited) obeys the following master equation (ME):[17]

$$\frac{\mathrm{d}}{\mathrm{d}t}P_i = -\left(\tau^{-1} + \sum_{j\neq i} W_{i\to j}\right)P_i + \sum_{j\neq i} W_{j\to i}P_j \qquad (4)$$

This system of coupled linear MEs can be solved by substituting into (4) $P_i(t) = C_i\exp(-\lambda t)$ with $\lambda > 0$, which leads to the eigenvalue problem of a real symmetric matrix (since the particles are considered identical, $W_{i\to j} = W_{j\to i}$). After finding the eigenvalues and the eigenvectors, one can obtain all $P_i(t)$ and then calculate the average polarization, $P(t) = \langle P_i(t)\rangle$, for any defined initial conditions. The emission intensity collected from a part of the area (A) of the dendrite is given by

$$I(t) = \text{const} \times P(t)/\tau \qquad (5)$$

where the average is taken over the area A. Note that, if the distances are measured in units of the particle size (R) and time in units of τ, a single parameter in our model is the dimensionless Förster radius, R_F/R.

As initial conditions mimic the experiment, some $N_0 \sim 10^2$ particles located within a circle with the center at a point (x_0, y_0) are excited, *i.e.*, for these particles $P_i(0) = 1$. For the nonexcited particles $P_i(0) = 0$. Then the whole system was allowed to evolve according to the MEs and the emission kinetics, $I(t)$, was "measured" for the N_0 particles within the collection spot. After processing these decay kinetics in the same way as the experimental data, we obtained simulated intensity and lifetime maps. A set of lifetime maps obtained for different values of the parameter R_F/R is shown in Fig. 6.

As can be seen from Fig. 6, for a very small Förster radius, the lifetime is longer at the ends of the dendrite, *i.e.* the excitation is localized there and no significant energy transfer takes place. However, for $R_F/R = 5$ the excitation is clearly funnelled into the centre of the structure. This is in agreement with our experimental findings for hybrid aggregates and can be understood by the anisotropy of the energy fluxes in a fractal structure where the density decreases from the centre towards the periphery.

FRET processes in ensembles of closely spaced QDs have been demonstrated in a number of previous studies.[18–23] In particular, it has been shown[9,10] that the optical properties of some QD dendrite structures suggest the occurrence of the non-radiative energy transfer from the photoexcited periphery to the dendrite core. However, in the present work we did not observe any significant spatial variations in the PL kinetics for dendritic structures consisting of solely QDs of the (nominally) same size. In fact, most clearly the evidence of FRET was shown for QD ensembles of two different sizes, where the roles of donors and acceptors are clearly distributed between the two QD species.[24] In our case, we expected that the transfer processes would be reversible (forward and back transfer should be possible), so

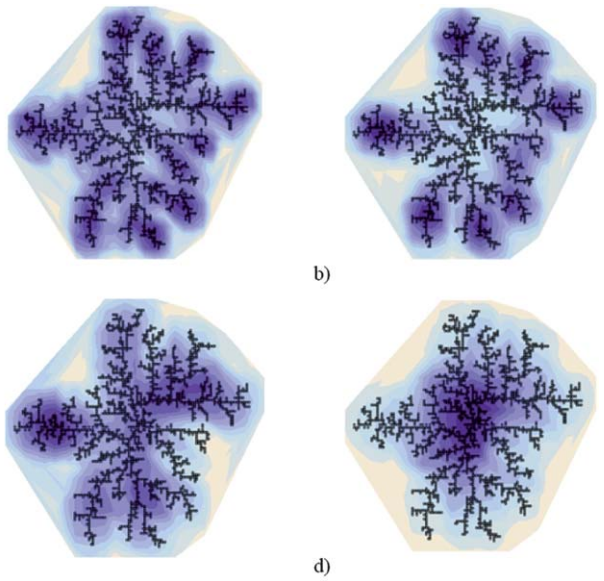

Fig. 6 Calculated PL lifetime maps for $R_F/R = 2$ (a), 3 (b), 4 (c) and 5 (d). Darker colour corresponds to a longer lifetime.

that each particle could act as both a donor and an acceptor. Indeed, our numerical model assuming the reversible transfer between identical particles forming a fractal (DLA) cluster can yield inhomogeneous distributions of the lifetime, which are the result of anisotropic energy fluxes in a system of variable particle density. The reason why it is not seen in our experiments with pure QD dendrites could be too broad a size distribution of QDs. When two neighboring dots have sizes different by just 10%, they are "disconnected" in terms of FRET.

In contrast, for the hybrid organic/inorganic structures of QDs and J-aggregates, we clearly observed changes in the lifetime distribution from the periphery of the dendrite to its center. We have shown that J-aggregates can be pumped indirectly, *via* QDs, in the spectral region where they do not absorb light. Furthermore, the longer PL lifetimes in the dendrite core, compared to its periphery, are indicative of long range non-radiative transport of energy as evidenced by our numerical modeling for the case of a sufficiently large Förster radius (>5 times the QD radius). We are not completely sure how this transport proceeds, *i.e.* what exactly are the absorbing/emitting "particles" in our model. Since pure QD aggregates do not show energy transport effects, we have two possibilities: (i) the energy transport takes place *via* J-aggregates that are initially excited *via* QDs or (ii) the "particles" in our model are coupled QD/J-aggregate complexes that act as both donors and acceptors. Although some further investigation is required to clarify this point, we can conclude that the hybrid QD/J-aggregate system possessing highly efficient energy transfer along with the capability to form a different type of dendritic structure is very promising for nanoelectronic and optoelectronic devices as well as renewable energy applications, where QD/J-aggregate dendritic structures could work as extremely efficient artificial light-harvesting and light-emitting systems.

Conclusions

In summary, we have studied the energy transfer processes in dendrite structures formed from spontaneously assembled CdTe QDs and J-aggregates of cyanine dye. Our results demonstrate that the energy fluxes to and from the centre of the structure, where the QD density is higher than that in the periphery of the dendrite, can be only observed when dendrites are formed from NCs integrated with J-aggregates but not in the case of structures formed from QDs of similar sizes alone. Comparison with the theoretical modeling results indicates that the anisotropy in the FRET-based fluxes to and from dendrites' center are related to the fractal topology of the structure, with the donor/acceptor density decreasing from the center to the periphery. Moreover, it requires a sufficiently large Förster radius to take place.

Acknowledgements

This research was supported by the ETORTEK 2011–2013 project "nanoIKER" from the Department of Industry of the Basque Government and by the Ministry of Education and Science of the Russian Federation Contract no. 8842 and 11.G34.31.0050. Financial support from the Portuguese Foundation for Science and Technology (FCT) and FEDER through Projects PTDC-FIS-113199-2009 and PEst-C/FIS/UI0607/2011 is gratefully acknowledged.

References

1 C. B. Murray, C. R. Kagan and M. G. Bawendi, *Science*, 1995, **270**, 1335–1338.
2 G. M. Whitesides and B. Grzybowski, *Science*, 2002, **295**, 2418–2421.
3 Z. Tang, N. A. Kotov and M. Giersig, *Science*, 2002, **297**, 237–240.
4 Y. P. Rakovich, F. Jackel, J. F. Donegan and A. L. Rogach, *J. Mater. Chem.*, 2012, **22**, 20831–20839.
5 Q. Zhang, T. Atay, J. R. Tischler, M. S. Bradley, V. Bulovic and A. V. Nurmikko, *Nat. Nanotechnol.*, 2007, **2**, 555–559.
6 B. J. Walker, G. P. Nair, L. F. Marshall, V. Bulovic and M. G. Bawendi, *J. Am. Chem. Soc.*, 2009, **131**, 9624–9625.
7 D. Savateeva, D. Melnikau, V. Lesnyak, N. Gaponik and Y. P. Rakovich, *J. Mater. Chem.*, 2012, **22**, 10816–10820.
8 V. M. Agranovich, Y. N. Gartstein and M. Litinskaya, *Chem. Rev.*, 2011, **111**, 5179–5214.
9 A. Sukhanova, A. V. Baranov, T. S. Perova, J. H. M. Cohen and I. Nabiev, *Angew. Chem., Int. Ed.*, 2006, **45**, 2048–2052.
10 V. E. Adrianov, V. G. Maslov, A. V. Baranov, A. V. Fedorov and M. V. Artemyev, *J. Opt. Technol.*, 2011, **78**, 699–705.
11 H. Sun, H. Wei, H. Zhang, Y. Ning, Y. Tang, F. Zhai and B. Yang, *Langmuir*, 2010, **27**, 1136–1142.
12 A. L. Rogach, T. Franzl, T. A. Klar, J. Feldmann, N. Gaponik, V. Lesnyak, A. Shavel, A. Eychmüller, Y. P. Rakovich and J. F. Donegan, *J. Phys. Chem. C*, 2007, **111**, 14628–14637.
13 V. Lesnyak, N. Gaponik and A. Eychmuller, *Chem. Soc. Rev.*, 2013, **42**, 2905–2929.

14 B. Mandelbrot, *The Fractal Geometry of Nature*, W. H. Freeman and Co., New York, 1982.
15 X. Wang, L. Qu, J. Zhang, X. Peng and M. Xiao, *Nano Lett.*, 2003, **3**, 1103–1106.
16 T. A. J. Witten and L. M. Sander, *Phys. Rev. Lett.*, 1981, **47**, 1400–1403.
17 J. P. S. Farinha and J. M. G. Martinho, *J. Phys. Chem. C*, 2008, **112**, 10591–10601.
18 C. W. Chen, C. H. Wang, Y. F. Chen, C. W. Lai and P. T. Chou, *Appl. Phys. Lett.*, 2008, **92**, 051906.
19 V. Rinnerbauer, H. J. Egelhaaf, K. Hingerl, P. Zimmer, S. Werner, T. Warming, A. Hoffmann, M. Kovalenko, W. Heiss, G. Hesser and F. Schaffler, *Phys. Rev. B: Condens. Matter Mater. Phys.*, 2008, **77**, 085322–085329.
20 E. Mutlugun, P. L. Hernandez-Martinez, C. Eroglu, Y. Coskun, T. Erdem, V. K. Sharma, E. Unal, S. K. Panda, S. G. Hickey, N. Gaponik, A. Eychmüller and H. V. Demir, *Nano Lett.*, 2012, **12**, 3986–3993.
21 M. Lunz, A. L. Bradley, W.-Y. Chen, V. A. Gerard, S. J. Byrne, Y. K. Gunko, V. Lesnyak and N. Gaponik, *Phys. Rev. B: Condens. Matter Mater. Phys.*, 2010, **81**, 205316.
22 M. Lunz, A. L. Bradley, V. A. Gerard, S. J. Byrne, Y. K. Gun'ko, V. Lesnyak and N. Gaponik, *Phys. Rev. B: Condens. Matter Mater. Phys.*, 2011, **83**, 115423.
23 A. L. Rogach, *Nano Today*, 2011, **6**, 355–365.
24 C. R. Kagan, C. B. Murray and M. G. Bawendi, *Phys. Rev. B: Condens. Matter Mater. Phys.*, 1996, **54**, 8633–8643.